



HAL
open science

3D-FSS Unit-Cell Simplification and Modelling for Single-Polarized Wideband Bandpass Applications

Paul Le Bihan, Raphaël Gillard, Erwan Fourn, María Garcia Vigueras, Isabelle Le Roy-Naneix, Stefan Varault, Christian Renard

► **To cite this version:**

Paul Le Bihan, Raphaël Gillard, Erwan Fourn, María Garcia Vigueras, Isabelle Le Roy-Naneix, et al.. 3D-FSS Unit-Cell Simplification and Modelling for Single-Polarized Wideband Bandpass Applications. 2021 IEEE Conference on Antenna Measurements & Applications, Nov 2021, Antibes Juan-Les-Pins, France. hal-03509385

HAL Id: hal-03509385

<https://hal.science/hal-03509385>

Submitted on 4 Jan 2022

HAL is a multi-disciplinary open access archive for the deposit and dissemination of scientific research documents, whether they are published or not. The documents may come from teaching and research institutions in France or abroad, or from public or private research centers.

L'archive ouverte pluridisciplinaire **HAL**, est destinée au dépôt et à la diffusion de documents scientifiques de niveau recherche, publiés ou non, émanant des établissements d'enseignement et de recherche français ou étrangers, des laboratoires publics ou privés.

3D-FSS Unit-Cell Simplification and Modelling for Single-Polarized Wideband Bandpass Applications

LE BIHAN Paul
THALES DMS France
Elancout (78), France
paul.lebihan@fr.thalesgroup.com

GILLARD Raphaël
INSA Rennes
Rennes (35), France
raphael.gillard@insa-rennes.fr

FOURN Erwan
INSA Rennes
Rennes (35), France
erwan.fourn@insa-rennes.fr

GARCIA VIGUERAS María
INSA Rennes
Rennes (35), France
garia.garcia-vigueras@insa-rennes.fr

LE ROY NANEIX Isabelle
THALES DMS France
Elancout (78), France
isabelle.leroyaneix@fr.thalesgroup.com

VARAULT Stefan
THALES DMS France
Elancout (78), France
varault.stefan@fr.thalesgroup.com

RENARD Christian
THALES DMS France
Elancout (78), France
renard.christian@fr.thalesgroup.com

Abstract— This paper proposes a novel 3D-FSS structure, which exhibits a wideband (~60%) and sharp roll-off bandpass response for linear, single-polarized applications. A modification of a Waveguide Integrated Resonator unit-cell previously presented in literature is here introduced, which guarantees its original overall filtering properties while simplifying its geometry. An equivalent electrical circuit model of the proposed structure is presented for a normal incidence case. As its results are validated through fullwave simulations, they both confirm hypotheses suggested on this novel unit-cell and consolidate the general knowledge on the working principles of this family of structures.

Keywords — FSS, 3D-FSS, Periodic structure, Equivalent circuit model, Wideband, Filter.

I. INTRODUCTION

Frequency Selective Surfaces, also called FSS, have been the subject to wide studies for the past decades, as a useful way to synthesize filtering functions in free-space [1]. This concept is based on the use of periodic arrays of subwavelength elements called unit-cells. As an impinging incident wave hits such an array, it is partially reflected or transmitted through it. This amount of transmitted power directly depends on the unit-cell properties: its geometry, its periodicity and the materials it is composed of. It is also affected by the angle of incidence of this impinging wave.

The capability to achieve filtering functions with a low profile raised a significant emphasis in the design of 2D-FSS radomes or sub-reflectors [2-4], for instance. However, 2D-FSS arrays made out of planar conducting elements also present limitations regarding bandwidth and oblique incidence stability. Indeed, they usually involve resonant elements (typically printed loops or patches) with very selective but narrow-band filtering responses [5]. On the other hand, such 2D geometries do not offer enough degrees of freedom to synthesize complex filtering response. Several principles have been proposed to address these issues, such as convoluting conductive elements to reduce periodicity [6], or stacking multiple FSS to increase the filtering response order [7]. Nevertheless, for this last alternative, the manufacturing cost and bulkiness dramatically increase with the number of involved substrate layers.

In the recent years, novel periodic structures concept has emerged from literature, not relying on two- but on three-dimensional unit-cells. Their geometry does not consist of printed substrates but involves actual volume structures. Thus, many examples of so-called 3D-FSS have been proposed, showing a rich diversity of geometries. Compared to traditional 2D-FSS, this type of structure shows potential benefits in terms of bandwidth [8], angular stability [9, 10], dual-polarization [11] or reconfiguration capability [12]. Indeed, the access to a supplementary dimension multiplies the possible degrees of freedom and also makes the miniaturization of the unit-cell easier [9]. New concepts may then be envisaged. In particular, as highlighted in [8], 3D unit-cells may involve simultaneous different parallel paths to transmit an incoming wave, with the potential to achieve selective and wideband response, whereas conventional 2D unit-cells are more likely assimilated to a single transmission path made of cascaded elements.

While it is worth to note that progress in additive manufacturing actually pushes forward these new concepts [9, 10, 12], a significant amount of 3D-FSS also takes advantage from more traditional technologies, such as printed circuit boards [8, 11]. Whatever the fabrication technique, 3D-FSS require complex manufacturing processes, which drastically limits the spreading of their use in practical applications. Thus, significant advantages can be taken from the emergence of simplest designs to reduce fabrication complexity while preserving the benefits of 3D geometries.

In such a context, this contribution proposes a new 3D-FSS. It is inspired from the structure introduced by Pelletti *et al* in [13], which shows sharp roll-off and wideband bandpass response for dual-polarization applications. The proposed unit-cell in this paper significantly reduces the complexity of the original one, making it feasible for realistic applications. The demonstration is done here for a single polarization and directly derives from the Waveguide Integrated Resonator we proposed in [14].

This paper is then organized as follows: Section II-A describes the proposed unit-cell geometry. Section II-B reminds previous developments on WIR structures and lists difficulties which can be encountered while dimensioning such 3D-FSS. Section III-A then introduces the approach

from which is derived the proposed structure. An equivalent electrical circuit of this novel unit-cell is introduced, in the case of normal incidence. This model provides physical insights on the electromagnetic behavior of the proposed solution, with regards to the knowledge of previous WIR unit-cells. The validity of this circuit is finally verified by comparison with fullwave simulations in Section III-B.

II. WIR-BASED UNIT-CELL PROPOSAL

A. Description of the proposed unit-cell

The structure proposed in this paper is presented in Fig. 1. It is here supposed to be the unit-cell of a two-dimensional periodic array placed in the (x,y) plane, excited by a y -polarized incident wave propagating in the z direction. As can be observed, it consists of two perfectly conducting sub-elements embedded into a thick substrate of dielectric permittivity ϵ_r : one folded wire resonator (in blue), and a pair of y -oriented strip lines (in dark green). The width of the strip lines is w , and their separation distance is $D-2w$. They are located at half the depth of the substrate core, *i.e.* at $z = h/2$ (h being the substrate thickness). The resonator is folded in the (y,z) plane and is made out of 3 segments: a central z -oriented segment of length l_z and two identical y -oriented arms of length l_y which can be excited by a vertically-polarized incident electric field.

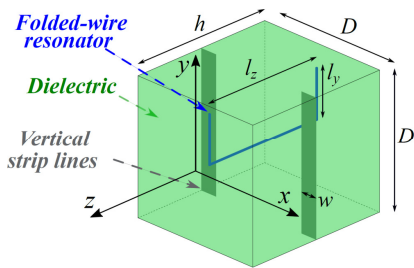


Fig. 1. Proposed WIR-based unit-cell.

B. Comparison with previous WIR structures

The unit-cell proposed in Fig.1 actually reveals strong similarities with the WIR structures studied in [13-15] (recalled in Fig.2(a-c)), whose electromagnetic behavior exhibit promising performances for linearly polarized applications with high out-of-band rejection, sharp roll-off and bandpass nature reaching 66%. While these WIR structures also use folded-wire resonators, these ones are integrated in a square metallic waveguide. The original WIR structure (Fig.2(a), [13]) is composed of four wire resonators: two of them are folded along the y -axis in order to be polarized by y -polarized incident wave, while the other ones are folded along the x -axis to be polarized by a x -polarized incident wave. As this unit-cell presents a geometrical symmetry by a 90° rotation around the z -axis, it behaves similarly when exposed to a vertically- or horizontally-polarized impinging wave under normal incidence.

The modified unit-cell in Fig.2(b) has been studied in [14]. It derives from the original WIR structure (Fig.2(a)), but simplifications have been done so that it only works for a y -polarized impinging wave. This simplified unit-cell thus consists of a single pair of y -polarized resonators embedded into a square metallic waveguide. In [14], an equivalent circuit was proposed for such a structure under normal incidence, highlighting the relationship between its geometrical parameters and the obtained filtering response.

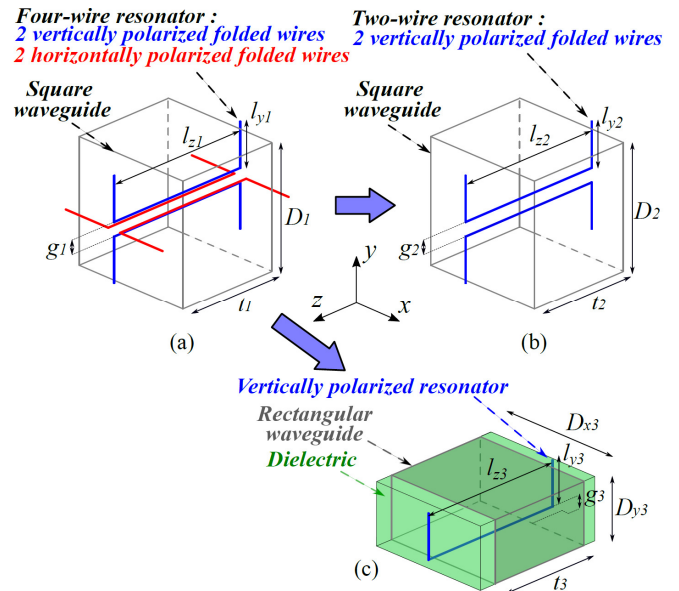


Fig. 2 WIR unit-cell variants proposed in the literature: [13] (a), [14] (b), [15] (c).

As another step to the simplification of WIR unit-cells for single-polarized applications, benefits taken from the symmetry of excitation regarding geometry led to the unit-cell proposed in [15] (Fig. 2(c)), ending up with a single wire resonator embedded inside a dielectric loaded rectangular waveguide.

Despite all these successive simplifications, WIR variants for single-polarized needs still suffer from a significant geometrical complexity. The first constraint to be encountered is due to the presence of the square metallic waveguide. Indeed, its cross-section controls both the periodicity of the unit-cell (and consequently the onset of higher-order Floquet modes [1]), but also the cut-off of the waveguide modes. Moreover, the dimensions of this geometry, particularly the thickness of its metallic walls, may have a strong impact on its coupling with the impinging wave. It was also demonstrated in [14] that the dimensioning and positioning of WIR's resonator in the waveguide was highly critical for the final filtering performance. The second constraint to be noted results from the dielectric loading. Although it is necessary to enable the propagation of the fundamental waveguide mode while preventing for the excitation of higher-order Floquet modes in the FSS, it makes the integration of the WIR even more difficult [15]. As a result, intractable tradeoffs between the different dimensions have to be achieved, making the design procedure a very difficult task. Face to these issues, the solution proposed in the present work (Fig. 1) relies on the suppression of the waveguide and its replacement by a planar grid of strip lines.

III. PHYSICAL INTERPRETATION OF THE PROPOSED SOLUTION

A. Equivalent electrical circuit modelling proposal

As mentioned in Section II-B, an equivalent circuit model has been proposed for the simplified WIR structure in [14]. From a physical point of view, it underlines the working principle of WIR structures as two parallel paths offered to the wave to propagate through the unit-cell. As also discussed in the previous section, the waveguide plays a significant role in the WIR mechanism as a highpass filter, which cutoff frequency is ideally located in the center of the unit-cell bandpass response [14]. The solution proposed in Fig. 1 relies

on the use of a grid of metallic strips instead. As demonstrated in [16], such strips produce an inductive behavior effect when excited by a parallel electric field and a highpass response can then be obtained. From the modelling point of view, the proposed electrical circuit of the new unit-cell is shown in Fig. 3, which is composed of two branches in parallel. Each of them is connected at both ends to a transmission line of length $(h-l_z)/2$, propagation constant $k_r = k_0\sqrt{\epsilon_r}$ and impedance $\eta_r = \eta_0/\sqrt{\epsilon_r}$. These lines are terminated by a port of impedance η_0 . As these two ports represent the free-space propagation at the front and rear of the unit-cell, the transmission lines account for the substrate interspace between free-space and the folded ends of the wire resonator.

The lower branch of the circuit represents the folded resonator. It consists of three transmission lines surrounded by reactive components. They account for the coupling of the resonator with the excitation. The central transmission line of this branch represents the z -directed section of the resonator. Its propagation constant and impedance are noted η_r and k_r , as it is fully embedded into the substrate core of the unit-cell. The two external transmission lines then represent the y -oriented ends of this wire. As these sections are typically placed near the interface between the substrate and free-space, they are here subject to an effective propagation constant and impedance, namely $k_{reff} = k_0\sqrt{\epsilon_{reff}}$ and $\eta_{reff} = \eta_0/\sqrt{\epsilon_{reff}}$. ϵ_{reff} defines an effective constant equal to $\sqrt{\epsilon_r + 1}/2$. The length of these three transmission lines is defined by their physical dimensions l_y and l_z , which are affected by a tuning parameter r . It accounts for right angle bends along the wire, which affect its overall electrical length. Both ends of the lower branch consist in a serial LC cell, which reactive components are respectively noted L_{res} and C_{res} . These elements represent the coupling of the y -polarized ends of the resonator at its two access.

The upper branch of the circuit is composed by a central reactive component noted Z_{strip} , surrounded by two transmission lines. While Z_{strip} represents the inductive behavior generated by the strip lines in the center of the unit-cell, the two transmission lines of length $h/2$, propagation constant k_r and impedance η_r , here model the dielectric slabs into which this grid is embedded.

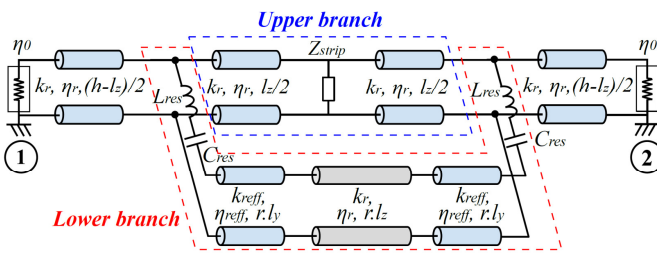


Fig. 3. Electrical equivalent circuit of the structure proposed in Fig. 1 for normal incidence.

The equivalent circuit presented in Fig. 3 also underlines the similarities between the structure proposed in this paper and the WIR studied in [14]. Indeed, regardless of the dielectric loading, these circuits present the same topology. The lower branch, representing the resonator, here remains similar, as the geometry of this element is unchanged. The upper branch of the circuit then illustrates the main difference between these 3D-FSSs, with the strip line impedance Z_{strip} replacing the waveguide and ensuring the highpass function.

B. Validation of the proposed unit-cell and its equivalent circuit model

A X-band bandpass structure is considered as an example, which central frequency is 9 GHz. The geometrical parameters are summarized in Table I. While the different segments of the resonator are here made out of cylindrical wires of a 0.1 mm diameter, the strip lines are supposed to be composed of 0.035 mm thick metallic plates (in the z -axis). The dielectric material constant of the substrate is $\epsilon_r = 3.475$.

TABLE I. GEOMETRICAL PARAMETERS (MILLIMETERS)

D	h	w	l_z	l_y
7.941	7.738	1.305	6.714	4.434

The validation of the equivalent electrical circuit presented in Fig. 3 is based on the same approach than the one proposed in [14], with the separated analysis of the folded-wire resonator and the strip lines. First, the analysis of the resonator is based on the unit-cell presented in Fig. 1, from which the strip lines are removed. Its equivalent circuit can be derived from Fig. 3, with the suppression of the Z_{strip} lumped impedance in the upper branch (framed in blue). The remaining component of this branch thus resumes in a single transmission line of length l_z , propagating constant k_r and impedance η_r . It represents the wave propagation through the overall dielectric slab between the two folded arms of the resonator. Coupling parameters, *i.e.* L_{res} , C_{res} and r , are extracted from curve-fitting between the computed results of the equivalent circuit and a fullwave simulation of the resonator under a normal incidence. Considering dimensions of Table I, L_{res} , C_{res} and r are here respectively estimated to 2.4 nH, 40.66 fF and 0.71. As illustrated in Fig. 4, a strong agreement between S-parameters obtained from such circuit and fullwave simulation is observed from zero to 14 GHz. The unit-cell periodicity D implies a grating lobes onset at 37.8 GHz under normal incidence [1], which is far above the observed bandwidth. As experienced in [14], the loss of accuracy observed in this model from 14 GHz can be explained by the approximation used in this representation of coupling : parameters L_{res} , C_{res} and r are supposed to be constant, which is a bit simplistic for such a large frequency band.

Concerning the strip line modelling, one can take example of the unit-cell presented in Fig. 1, where the resonator element is removed and replaced by dielectric substrate. From Fig. 3, the equivalent circuit of strip lines leads to the suppression of the lower branch. It then resumes in a lumped impedance Z_{strip} , surrounded by two transmission lines representing the half dielectric slabs into which it is embedded. The length, propagation constant and impedance of these transmission lines are respectively noted $h/2$, η_r and ϵ_r . The impedance Z_{strip} can be calculated in function of the dimensions of the strips from [16]. A comparison of this model with fullwave simulation, presented in Fig. 5, shows its relevance over the considered bandwidth, retrieving a highpass behavior.

Finally, Fig. 6 compares the response computed of equivalent circuit in Fig. 3 and a fullwave simulation of the proposed unit-cell. Strong agreements are here found, both demonstrating the capability of this 3D-FSS to replicate the response of WIR-based structures, and the working principle assumptions presently made. Above 12 GHz, the accuracy of this equivalent circuit appears to decrease, which can be

explained by several factors. As previously discussed, the progressive drift of the resonator's parameters with frequency, *i.e.* L_{res} , C_{res} and r , may directly contribute to these differences. Furthermore, it can be noticed that the circuit proposed in Fig. 3 does not account for reactive couplings between the resonator and the inductive strips, which also affects the response of the unit-cell as frequency varies. Despite these facts, the global response of this structure is reproduced, with the prediction of its different transmission poles and zeroes up-to 20 GHz.

Beyond the validation of this circuit, the interest of strip lines as a substitute to waveguide is also confirmed by these results. Indeed, as can be noted from [16], strip line impedance Z_{strip} is defined by the couple of values (D, w) . Thus, in the validity domain of this model, the periodicity of the unit-cell (D) can be independently chosen from the synthesized impedance by adjusting the width of the strip lines (w). In other words, this degree of freedom relieves the dependency previously experienced in the case of structures illustrated Fig. 2, between the unit-cell periodicity and the propagation properties of a waveguide. Furthermore, another significant

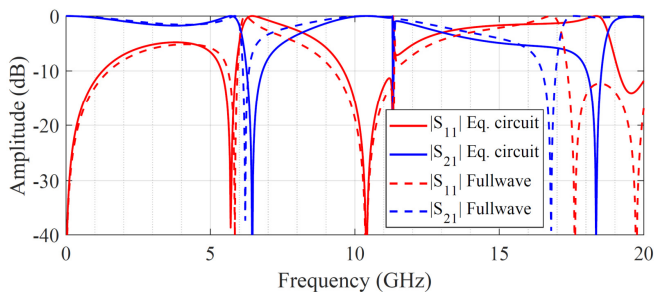


Fig. 4. S-parameters comparison between the fullwave simulation of the resonator embedded into dielectric slabs and its equivalent electrical circuit model.

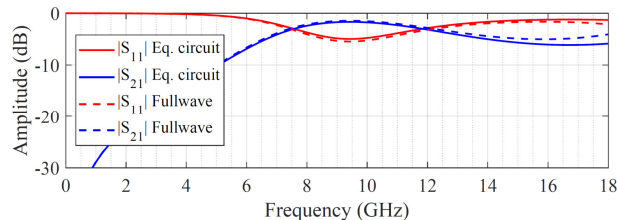


Fig. 5. S-parameters computed from fullwave simulation of the inductive strip lines embedded into dielectric slabs and its equivalent electrical circuit model.

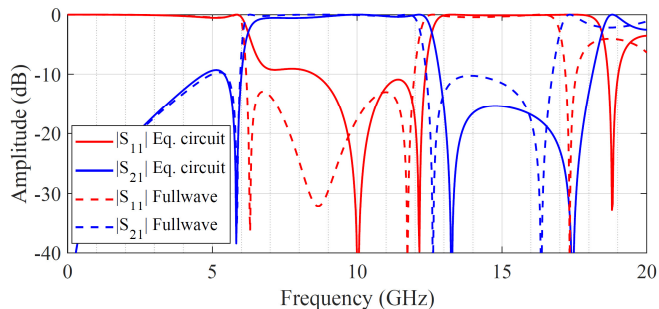


Fig. 6. S-parameters comparison between the proposed structure simulated through fullwave simulation and the equivalent electrical circuit proposed in Fig. 3.

benefit is obtained from this geometry: the presence of the inductive lines do not represent any obstacle (*i.e.* positioning constraint) to the resonator along the y -axis, which is then released from the presence of horizontal metallic walls.

IV. CONCLUSION

This paper presents a geometrical simplification of WIR 3D-FSS unit-cells previously proposed in the literature, while preserving their filtering performance for single, linearly-polarized applications. As the proposed 3D-FSS is firstly described, difficulties which can be encountered with previous WIR structures are discussed. From a modelling approach, its equivalent electrical circuit is introduced and validated through fullwave simulations, showing the relevance of the proposed concept. This contribution then relieves WIR-based unit-cells from geometrical constraints in the frame of wideband, bandpass filtering needs.

REFERENCES

- [1] B. A. Munk, "Frequency Selective Surfaces – Theory and Design", Wiley Interscience, 2000.
- [2] E. Pelton, B. A. Munk, "A Streamline Metallic Radome", IEEE TAP, vol. 22, No 6, 1974.
- [3] K. K. Varikuntla, R. S. Velu, "Design and Development of Angularly Stable and Polarization Rotating FSS Radome base on Substrate-Integrated Waveguide Technology", IET Microwaves, Antennas & Propagation, vol. 13, 2019.
- [4] M. L. Zimmerman *et al*, "Analysis of reflector antenna system including frequency selective surfaces", IEEE TAP, Vol. 40, No 10, 1992.
- [5] R. J. Langley, E. A. Parker, "Equivalent circuit model for arrays of square loops", Electronics Letters, Vol. 18, No 7, 1982.
- [6] E. A. Parker *et al*, "Convolved Dipole Array Elements", Electronics Letters, Vol. 27, No 4, 1991.
- [7] N. Behdad, M. A. Al-Joumayly, "A Generalized Synthesis Procedure for Low-Profile, Frequency-Selective Surfaces With Odd-Order Bandpass responses", IEEE TAP, Vol. 58, No 7, 2010.
- [8] A. Al-Sheikh, Z. Shen, "Design of Wideband Bandstop Frequency Selective Structures Using Stacked Parallel Strip Line Arrays", IEEE TAP, Vol. 64, No 8, 2016.
- [9] B. Sanz-Izquierdo, E. A. Parker, "Frequency Selective Surfaces Formed by Partially Metalizing 3D Elements", EuCAP, 2015.
- [10] J. Zhu *et al*, "Dual-Polarized Bandpass Frequency-selective Surface With Quasi-Elliptic Response Based on Square Coaxial Waveguide", IEEE TAP, Vol. 66, No 3, 2018.
- [11] J. Zhu *et al*, "A Dual-Polarized Bandpass Frequency Selective Surface With Stable Response", IEEE AWPL, Vol. 20, No 5, 2021.
- [12] S. A. Nauroze *et al*, "Inkjet-printed « 4D » tunable spatial filters using on-demand foldable surfaces", 2017 IEEE-MTS IMS, 2017.
- [13] C. Pelletti *et al*, "Frequency selective surface with wideband quasi-elliptic bandpass response", Electronics Letters, Vol. 49, No 17, 2013.
- [14] P. Le Bihan *et al*, "Modelling of a 3D Periodic Surface Based on a Folded Resonator Embedded into a Waveguide", 49th European Microwave Conference, 2019.
- [15] P. Le Bihan *et al*, "Three-Dimensional Frequency Selective Surface for Single-Polarized Filtering Applications with Angular Stability", 14th European Conference on Antennas and Propagation, 2020.
- [16] N. Marcuvitz, "Waveguide Handbook", McGraw-Hill Book Company Inc., 1st ed, 1951.